Int. Symp. on Heat Transfer in Gas Turbine Systems
9-14 August 2009, Antalya, Turkey

A CORRELATION-BASED METHODOLOGY TO PREDICT THE FLOW STRUCTURE OF FLOWS EMANATING FROM CYLINDRICAL HOLES WITH APPLICATION TO FILM COOLING

Tilman auf dem Kampe and Stefan Völker
Siemens AG, Energy Sector, Fossil Power Generation Division
Mellinghofer Str. 55, 45473 Mülheim a. d. Ruhr, Germany
tilman.aufdemkampe@siemens.com, voelker.stefan@siemens.com

EXTENDED ABSTRACT

Film cooling flows and the proper prediction of their cooling effect play an important role in today's gas turbine designs. Empirical correlations for laterally averaged film cooling effectiveness are commonly used to predict the cooling effect of the film. These correlations are applied along streamlines computed from CFD solutions of uncooled flow. However, this approach has some inherent flaws, such as neglecting the interaction between the emanating film cooling flows and the main flow in the 3D-CFD model or limited confidence in the applicability of correlations developed under experimental conditions to real engine flow situations with strong secondary flows. Baldauf [2001] has shown that film cooling effectiveness is influenced by a large number of parameters, not all of which are well-known when designing gas turbine components. A sensitivity study by auf dem Kampe and Völker [2009] shows that even the least significant parameters play an important role predicting film cooling effectiveness.

On the other hand, detailed modeling of film cooling holes in a 3D-CFD calculation with a sufficiently fine mesh to resolve the flow within the hole itself is not feasible in the design process of a gas turbine airfoil, as computational resources are limited and the required modeling effort is extremely high.

Despite the difficulties of developing correlations for film cooling effectiveness, auf dem Kampe and Völker [2009] argue that the near-hole flow structure of the exiting film-jet can very well be correlated based on the knowledge of only a few key flow parameters. Therefore, an approach to prescribe the flow structure in the region around the film hole exit within the 3D-CFD model promises to deliver improved results compared to the use of film effectiveness correlations, while at the same time not requiring abundant computational resources. Similar approaches have been proposed e.g. by Heidmann and Hunter [2001] and Burdet et al. [2005].

Table 1
Variation Intervals of Input Parameters

Parameter	Symbol	Definition	Variation Interval
blowing rate	M	$\rho_c u_c / \rho_\infty u_\infty$	$0.3 \ldots 2.0$
density ratio	DR	ρ_c / ρ_∞	$0.8 \ldots 2.0$
inlet Mach number	Ma	u_∞ / a_∞	$0.1 \ldots 0.5$
acceleration parameter	K	$\frac{\nu}{u^2}\frac{\partial u}{\partial s}$	$0 \ldots 5.0 \times 10^{-7}$
turbulence intensity	Tu	$\tilde{u}/u$	$0.01 \ldots 0.1$
inlet turbulent length scale	l_{turb}	$-$	$10\text{mm} \ldots 30\text{mm}$
compound angle	β	$-$	$0° \ldots 30°$

In this paper, correlations describing the complete three-dimensional flow field in the exit region of an inclined cylindrical film cooling hole are proposed. Based on a validated high-resolution CFD

model for a single cylindrical film cooling hole, numerical experiments have been conducted. Flow parameters summed up in Table 1 have been varied in the numerical experiments. The results from these numerical experiments serve as a data basis for the correlation development.

Jet-body envelope To describe a complex three-dimensional flow field in space through a set of mathematical formulae requires strong abstraction of the observed flow field. A step-by-step abstraction of the flow field based on mathematical and physical considerations is conducted. Free coefficients in the mathematical formulation allow for fitting these to results obtained from the numerical experiments. The fitted sets of coefficients are then correlated with the parameters in Table 1, thus providing a flow-parameter based capability for predicting the flow field of the exiting film-jet.

Due to the physics-based mathematical formulations, correlation-based estimates of the flow field are both robust and physically reasonable. Figures 2 and 3 both display data from the three steps of this process: CFD result, best fit of designed mathematical formulation to the CFD result, and correlation-based estimates.

The flow field is described in terms of the volume occupied by the film-jet exiting into the cross-flow boundary layer and the distribution of the momentum components within that volume.

The volume occupied by the exiting film-jet is described in terms of the envelope spanned by planes orthogonal to the film trajectory as indicated in Figure 1. For the film-jet trajectory a generalized solution is developed from a force-balance on an infinitesimally small section of the jet based on an approach presented by Abramovich [1963], see Equations 1 and 2 with $\varphi = y$, z and $\psi = \beta$, α respectively. In these equations A_φ, B_φ, φ_0, and ψ_{real} are free coefficients and thus flow-parameter-dependent functions, other unknowns are model constants.

$$\frac{\varphi}{d}\left(\frac{x}{d}\right) = \begin{cases} \frac{\varphi_0}{d} & | \, \psi < \psi_{min} \vee (\psi > \psi_{min} \wedge \psi_{real} < \psi_{min} \wedge x > x_0) \\ \tan\psi \, \frac{x}{d} & | \, \psi > \psi_{min} \wedge x < x_H \\ \frac{\varphi_M}{d} + \sqrt{\left(\frac{r_\varphi}{d}\right)^2 - \left(\frac{x-x_M}{d}\right)^2} & | \, \psi > \psi_{min} \wedge x_H \leq x \leq x_0 \\ f_{Abr,\varphi}\left(\frac{x}{d}\right) \text{ see Eq. 2} & | \, \psi > \psi_{min} \wedge \psi_{real} > \psi_{min} \wedge x > x_0 \end{cases} \tag{1}$$

$$f_{Abr,\varphi}\left(\frac{x}{d}\right) = \frac{\varphi_0}{d} + \sqrt{A_\varphi \frac{IR}{\sin\psi_{real}}} \cdot \ln\left[\frac{\sqrt{\left(\frac{x-x_0}{d}\right)^2 + 2\,B_\varphi \frac{x-x_0}{d} + A_\varphi \frac{IR\,\cot^2\psi_{real}}{\sin\psi_{real}}} + \frac{x-x_0}{d} + B_\varphi}{\sqrt{A_\varphi \frac{IR\,\cot^2\psi_{real}}{\sin\psi_{real}}} + B_\varphi}\right] \tag{2}$$

It is assumed that the shape of the cross-sections may be described by an asymmetric ellipsis centered about the origin of a coordinate system moving with the trajectory. The ellipsis is asymmetric in the sense that the length of the half axis in y^s-direction may differ in positive and negative y^s-direction (see Figure1).

The lengths of the half axes of the asymmetric ellipsis vary downstream after the film exits from the film hole and penetrates the cross-flow boundary layer. The observed behavior of the half axes plotted in Figures 2(c) and 2(d) can be described by a piecewise-linear approach given in Equation 3 where $m_{1,\varphi}$, $m_{2,\varphi}$, $x_{1,\varphi}$, and $x_{2,\varphi}$ are flow-parameter-dependent free coefficients, $b_{1,\varphi}$ and $b_{1,\varphi}$ follow from continuity constraints. As the film emanates from the hole, it begins to interact with the cross-flow boundary layer. Having an average momentum at an angle to the flow direction of the cross-flow, the film is bent and flattened by the cross-flow. The flattening deforms the jet-shape to the asymmetric elliptical shape. The extent of the jet-body in z^s-direction decreases while the extent in y^s-direction increases. At the same time, the film-jet is bent in the direction of the cross-flow. The bending and

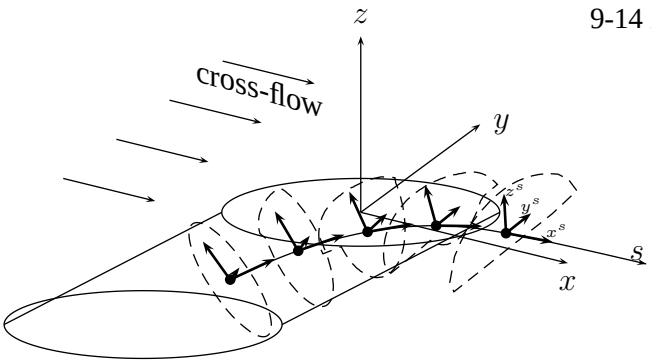

Figure 1: Trajectory and cross-sections of exiting jet-body

flattening of the jet is a phenomenon governed by the hydrodynamic interaction of jet and cross-flow. As film- and cross-flow-direction become approximately parallel, turbulent diffusion becomes the dominant mechanism, which gradually widens the jet body in all directions. These findings are summed up in Figure 2 which shows representative results from an arbitrarily chosen CFD run. The agreement between CFD result and correlation-based prediction is excellent.

$$\varphi = \begin{cases} \frac{d}{2} & | \, x < x_{1,\varphi} \\ m_{1,\varphi}\frac{x}{d} + b_{1,\varphi} & | \, x_{1,\varphi} \leq x \leq x_{2,\varphi} \\ m_{2,\varphi}\frac{x}{d} + b_{2,\varphi} & | \, x > x_{2,\varphi} \end{cases} \qquad \text{for} \quad \varphi = y^s_{max} \, , \; -y^s_{min} \, , \; z^s_{max} \tag{3}$$

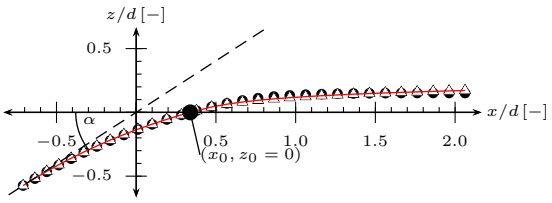

(a) Jet-trajectory in x-z-plane

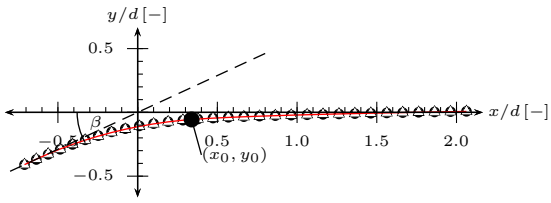

(b) Jet-trajectory in x-y-plane

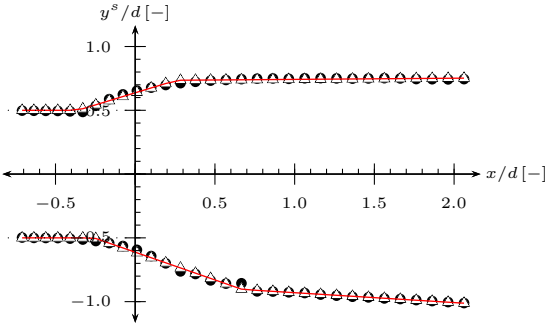

(c) Jet-body extents in y^s-direction

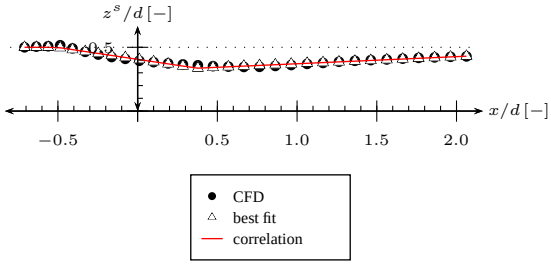

(d) Jet-body extent in positive z^s-direction

Figure 2: Correlations for abstracted volume formulations

Momentum distributions within jet-body Distributions of the momentum components are described in terms of two-dimensional distributions in cross-sections along the film-jet trajectory. The distributions are based on the well-researched counter-rotating vortex pair (CVP) emanating from inclined cylindrical film cooling holes observed by Leylek and Zerkle [1994]. As this is the dominant vortex structure of the jet, weaker vortex structures as described in detail by Vogel [1997] are not considered in the developed correlations.

Figure 3 shows a characteristic distribution of the velocity component in y^s-direction in a cross-section orthogonal to the hole axis, just before the film exits into the cross-flow boundary layer for an arbitrarily chosen CFD run. Velocity vectors indicate the orientation of the CVP. Again, the agreement between the CFD results, the best fit of the mathematical descriptions developed for these structures, and the correlation-based predictions is very good. Equations 4, 5, and 6 are the mathematical formulations used to describe the u^s, v^s, and w^s velocity components in local coordinates, where ξ and η denote normalized length parameters in y^s- and z^s-direction respectively.

$$u^s = f(\xi, \eta) \text{ (placeholder, elliptical transformation not yet completed)} \tag{4}$$

$$v^s = \frac{\cos\left[\frac{1}{2}\sqrt{2}\,(\xi+\eta)\right]}{1+\frac{1}{2}\,(\xi-\eta)^2} - \frac{\cos\left[\frac{1}{2}\sqrt{2}\,(\xi-\eta)\right]}{1+\frac{1}{2}\,(\xi+\eta)^2} \tag{5}$$

$$w^s = \frac{1}{2}\left(\frac{\cos\xi}{1+\eta^2}+1\right) \tag{6}$$

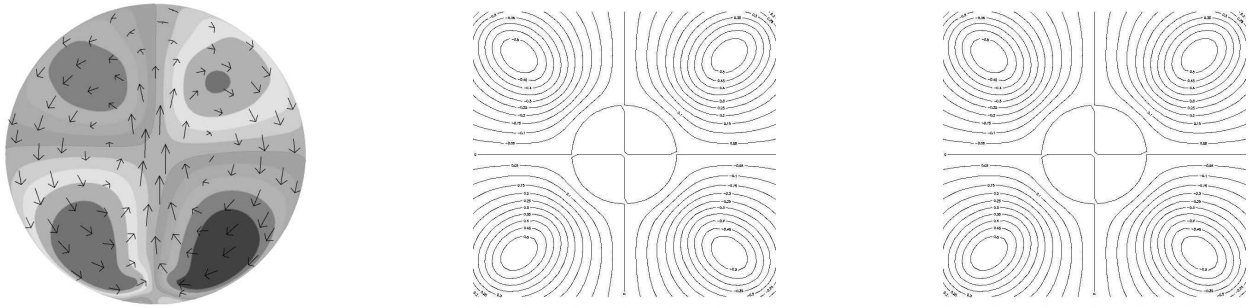

(a) CFD (b) best fit (placeholder) (c) correlation (placeholder)

Figure 3: Velocity component v^s in trajectory-orthogonal cross-section

REFERENCES

Abramovich, G. [1963]. *The Theory of Turbulent Jets*. The M.I.T. Press, Massachusetts Institute of Technology, Cambridge, Massachusets.

auf dem Kampe, T. G. and Völker, S. [2009]. Numerical Investigation of Flat Plate Film Cooling and Analysis of Variance of Relevant Flow Parameters. In F. Heitmeir, F. Martelli and M. Manna, editors, *8th European Turbomachinery Conference on Turbomachinery, Fluid Dynamics and Thermodynamics, 23-27 March 2009, Graz, Austria*, ETC8-123. pp. 569–578.

Baldauf, S. [2001]. Filmkühlung thermisch höchstbelasteter Oberflächen: Korrelation thermographischer Messungen. Ph.D. thesis, Universität Karlsruhe.

Burdet, A., Abhari, R. S. and Rose, M. G. [2005]. Modeling of Film Cooling - Part II: Model for Use in 3D CFD. In *Proceedings of GT2005, ASME Turbo Expo 2005: Power for Land, Sea and Air*. ETHZ.

Heidmann, J. D. and Hunter, S. D. [2001]. Coarse Grid Modeling of Turbine Film Cooling Flows Using Volumetric Source Terms. Technical Report NASA/TM-2001-210817, National Aeronautics and Space Administration (NASA).

Leylek, J. and Zerkle, R. [1994]. Discrete-Jet Film Cooling: A Comparison of Computational Results With Experiments. *Journal of Turbomachinery*, volume 116, no. 93-GT-207, pp. 358–368.

Vogel, D. T. [1997]. Numerische Untersuchung des Mischungsverhaltens von Filmkühlstrahlen in Turbinenströmungen. Ph.D. thesis, Ruhr-Universität Bochum.